Fig. 1. CryoEM structure of *E. coli* BAM in nanodiscs. A. The role of BAM in the biogenesis of b-barrel outer membrane proteins. Figure adapted from Imai *et al*., 2019. **B**. The procedure for forming BAM-inserted nanodiscs used for our EM studies. **C**. A representative SEC trace from the purification of BAM-inserted nanodiscs, along with SDS-PAGE gels for each of the purifications from our study. The black triangles indicate the nanodisc proteins. **D**. Negative-stain images for all BAM-inserted nanodisc samples in our study. The scale bars represent 50 nm. **E**. CryoEM reconstructions of BAM-inserted D1, E3, and N2 nanodiscs, including a top-down cutaway view of a superposition of the three structures showing nearly identical densities for each of the different nanodiscs used. The red dashed line indicates the location of the barrel domain of BamA, while the black dashed line indicates the perimeter of the nanodisc density. **F**. A refined model of BAM docked within the cryoEM 3D reconstruction of BAM in E3 nanodiscs at 4 Å resolution showing an outward-open conformation (red dashed lines), with an orthogonal view from the top of the barrel of BamA. **G.** Representative electron density for BamA (residues 600-620), BamB (residues 58-77), and BamD (residues 164-181).

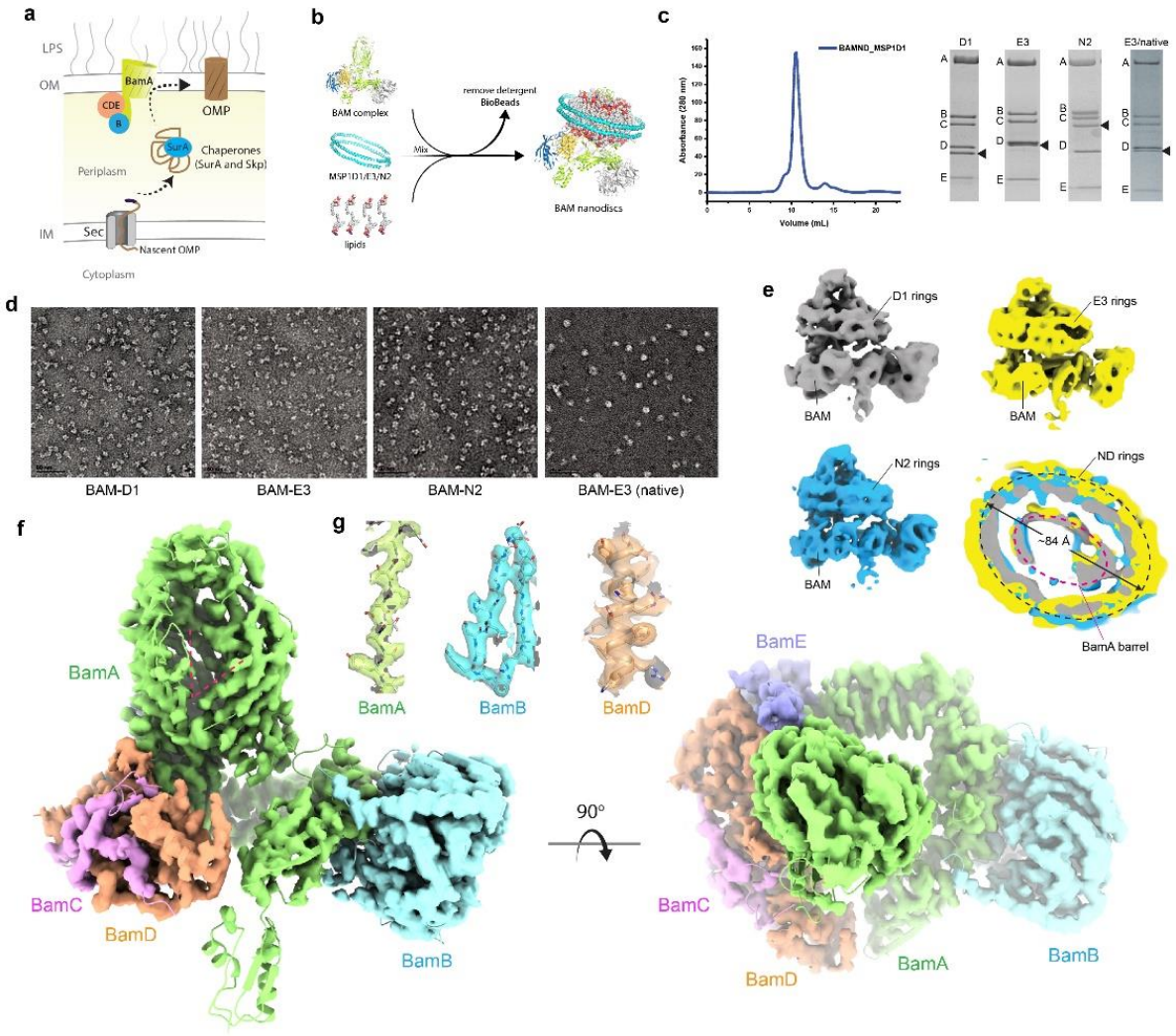

Fig. 2. Representative cryo-EM micrograph (A) and 2D classifications (B).

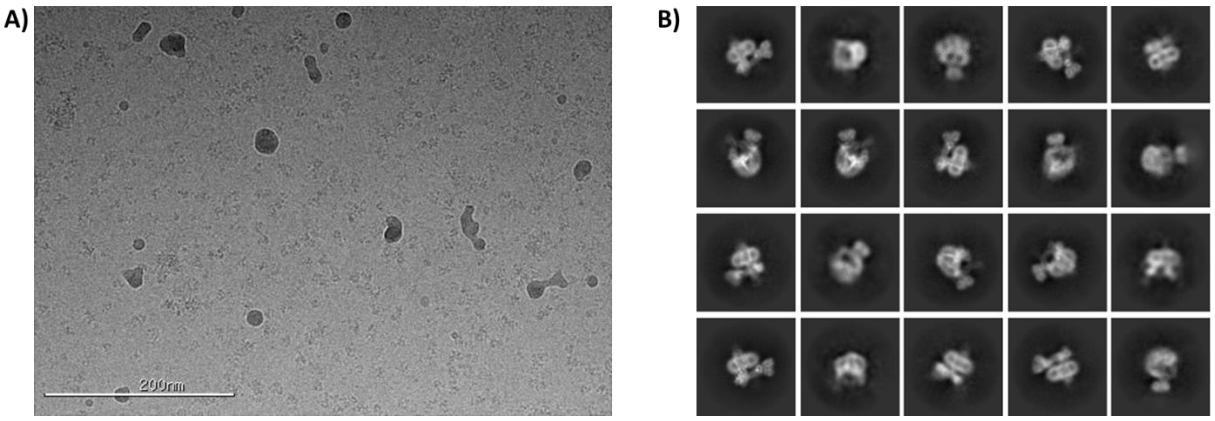

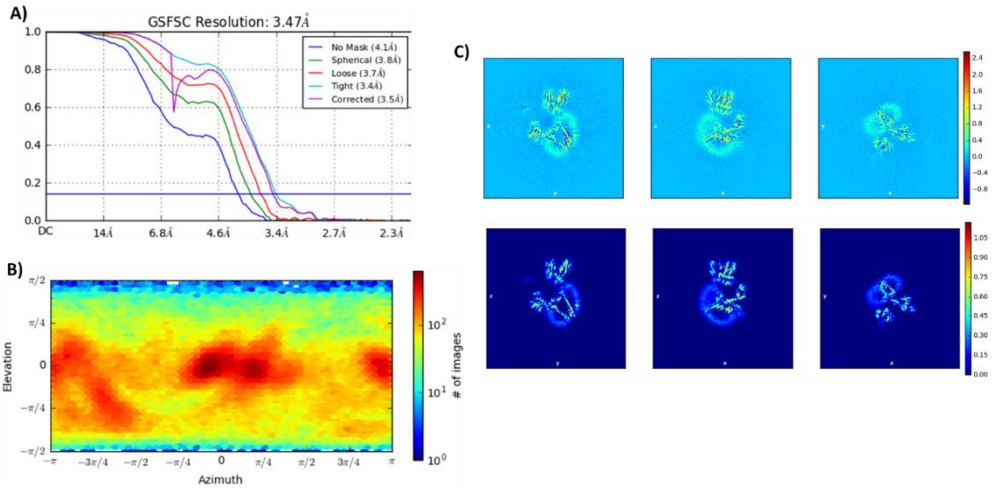

Fig. 3. (A) Gold standard FSC curves calculated with different masks in cryoSPARC, (B) Distribution of orientations over azimuth and elevation angles for particles used for the final map, (C) Real space slices without (upper) and with (bottom) masks after local refinement in cryoSPARC.

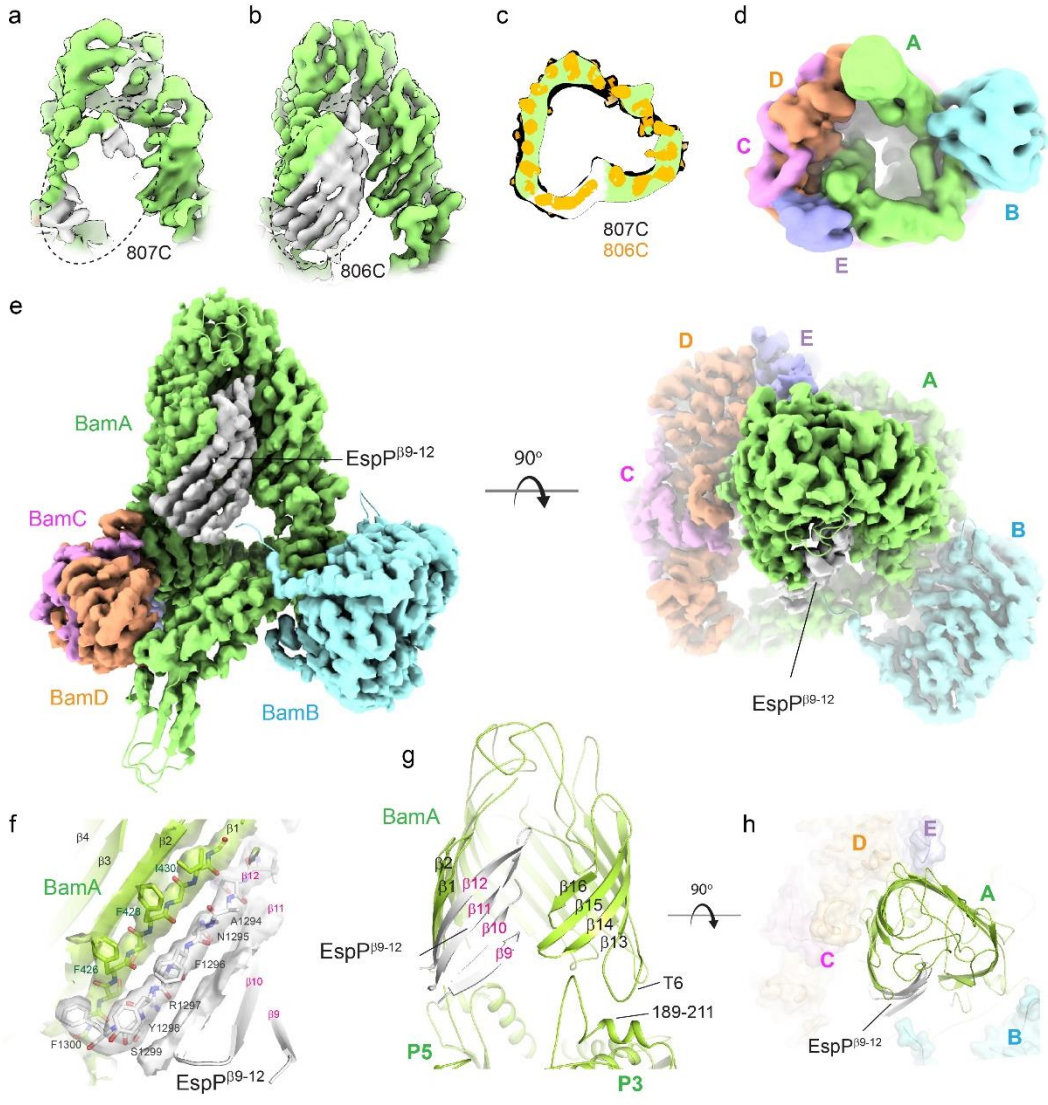

Fig.4. High resolution structure of the BAM/MBP-EspP^{b9-12} hybrid-barrel early intermediate. CryoEM map along the lateral seam within the BAM/MBP-EspP^{b9-12} structure with crosslinking between (**a**) residue 807 of b16 of BamA and residue 1226 of b9 of EspP and (**b**) residue 806 of b16 of BamA and residue 1226 of b9 of EspP. The dashed oval shows the increase in order observed with crosslinking at residue 806 of BamA. **c**. A top-down cutaway view comparing the non-sharpened map from panel **a** (green is the BamA barrel; white is EspP^{b9-12}) with the map in panel **b** (orange), depicting the same state observed for both crosslinking sites. **d**. A bottom view of a down-filtered map (7 Å) from panel **b**; no extra density is observed as was seen for the structure from the *in vitro* assay (Fig. 6f-i). **e.** Orthogonal views of the 3.4 Å resolution MBP-EspP^{b9-12} cryoEM map/structure showing the integration of EspP^{b9-12} within the expanded barrel of BamA, forming a hybrid-barrel early intermediate. The last strand of EspP^{b9-12} (b12) pairs with the first strand of BamA (b1). The N-terminal strands of EspP^{b9-12} then curve towards the inside of the barrel, which would assist in sealing the hybrid-barrel during biogenesis to maintain membrane integrity. **f**. Zoomed view of the four strands of EspP^{b9-12} integrated into the barrel of BamA. The density for b1 of BamA and b12 of EspP^{b9-12} is shown as transparent isosurface, allowing unambiguous assignment of the residues. **g**. View of the BamA/EspP^{b9-12} barrel with strand arrangements. The interaction between turn 6 (T6) and residues 189-211 of POTRA5 (P3) is shown which may stabilize the expansion of the C-terminal region of the BamA barrel during OMP biogenesis. **h**. Zoomed view of the triangular shape of BamA/EspP^{b9-12} hybrid-barrel, showing excellent agreement with the low resolution structure from Fig. 6j.